land

MDPI

Article

A Multi-Regional CGE Model for the Optimization of Land Resource Allocation: A Simulation of the Impact of High-Quality Development Policies in China

Luge Wen [1], Tiyan Shen [1,*] and Yuran Huang [2]

[1] School of Government, Peking University, Beijing 100871, China; wenluge@pku.edu.cn
[2] Beijing Municipal Finance Bureau, Beijing 101160, China; huangyuran35@163.com
* Correspondence: 2306394295@pku.edu.cn; Tel.: +86-182-1009-8691

Abstract: Land, as the foundation of all productive activities, plays a crucial role in achieving high-quality development across regions. China's current land allocation model, which focuses on land quota distribution, has several drawbacks and does not address the conflict between limited land availability and increasing demand. To maximize land use benefits, it is essential to develop scientifically sound allocation plans that effectively adjust land structure and layout. However, existing research often relies on single-attribute geographic or linear programming models which do not meet the multidimensional needs of modern territorial planning. Additionally, commonly used CGE models often overlook the critical role of construction land. To address these gaps, this study introduces a multi-scale, multi-type China Territorial Spatial Planning Simulation Model (CTSPM). This model integrates cultivated, forest, grassland, and construction land, simulating the land use changes driven by socioeconomic impacts through price mechanisms. By employing a land use transition matrix, the CTSPM enhances practical applicability and improves predictions for residential and non-agricultural construction land. It provides a scientific tool for evaluating land policies, supporting interdepartmental negotiations on land quotas, and contributing to natural resource governance and territorial spatial planning. Using the CTSPM, we simulated various high-quality development scenarios and derived the following conclusions: (1) An increase in Total Factor Productivity (TFP) significantly boosts regional economic development and the demand for non-agricultural land; a 1% increase in TFP leads to a 1.48% rise in actual GDP and a 0.19% increase in total non-agricultural land demand. (2) At the regional level, eastern regions experience a greater impact on total land demand compared to central and western regions. (3) In terms of land use types, cultivated and grassland areas show a decreasing trend, while forest and construction land areas are increasing.

Keywords: land resource allocation; China's territorial spatial planning policy; computable general equilibrium models; high-quality development; simulation model

Received: 13 January 2025
Revised: 9 February 2025
Accepted: 17 February 2025
Published: 21 February 2025

Citation: Wen, L.; Shen, T.; Huang, Y. A Multi-Regional CGE Model for the Optimization of Land Resource Allocation: A Simulation of the Impact of High-Quality Development Policies in China. *Land* **2025**, *14*, 450. https://doi.org/10.3390/land14030450

1. Introduction

The optimization of land allocation is of great significance to the realization of high-quality development of a whole region [1,2]. Since the reform and opening up, China's economy has developed rapidly, and the level of urbanization has also rapidly increased. From 1978 to 2020, China's average annual GDP growth rate increased to 12.07%, higher than the average growth rate of the United States (7%). Particularly since 2000, China's GDP growth rate has increased significantly at the same time as per capita GDP. China's per capita GDP in 2021 of 12,000 U.S. dollars exceeded the average 10,800 U.S. dollars of

middle-income countries. As can be seen in Figure 1, China's GDP growth has slowed or even declined since 2008, with the GDP growth rate falling from 10.64% in 2010 to 5.95% in 2019. China's economic development has entered a new normal as it has shifted from high to medium–high growth. The arrival of this new normal has prompted the economy to enter a new phase of transformation of its development model and growth pattern.

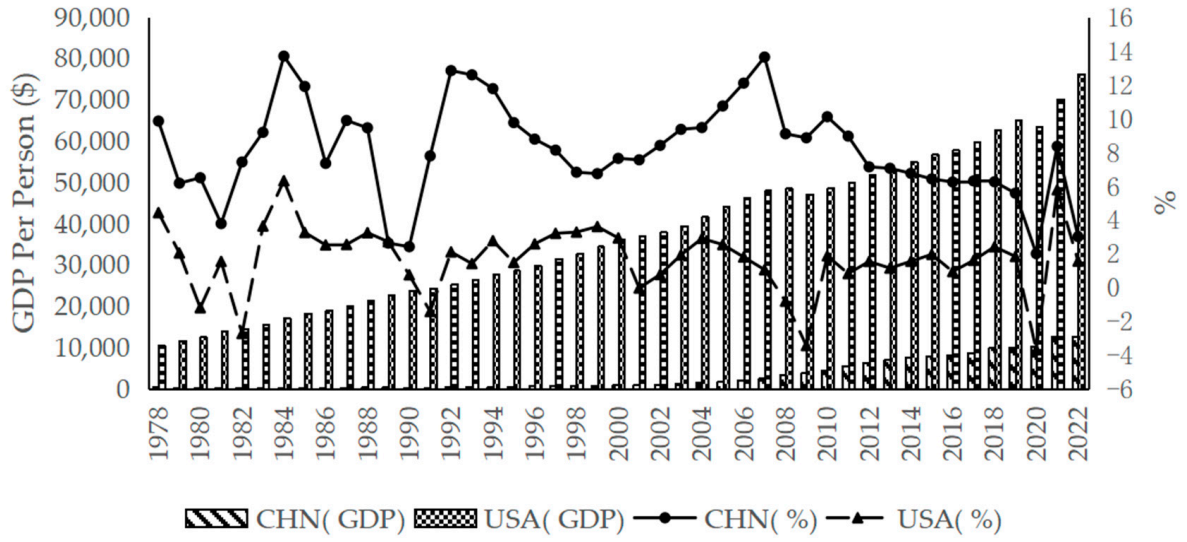

Figure 1. GDP per capita (US$) and GDP growth rates, China and the USA, from 1978 to 2021. Source: Authors' compilation based on World Bank database.

The report of the 19th National Congress of the Communist Party of China (CPC) notes that "China's economy has shifted from a stage of rapid growth to a stage of high-quality development", and the report of the 20th National Congress of the Communist Party of China states that "high-quality development is the primary task of building a modern socialist country in an all-round way". The report of the 20th Party Congress further pointed out that "high-quality development is the primary task of building a modern socialist country" and that "we should accelerate the construction of a new development pattern and strive to promote high-quality development". In the context of the new era, only higher quality, more efficient, fairer, and more sustainable development can cope with various risks and challenges [3]. However, with the rapid growth of China's economy, the problems of land use conflicts and ecological degradation have become more and more prominent, and the quality of land development is worrisome [4]. Land serves as the foundational platform and spatial conduit for coordinating diverse socioeconomic and ecological systems. This critical role renders land resource allocation a fundamental determinant in shaping regional development trajectories toward high-quality growth. Within China's governance framework, local governments operate as primary actors in land resource distribution, while the central government establishes nationwide land use masterplans and administers quota allocations through a top-down hierarchy to ensure coherent territorial spatial governance [5]. Consequently, the scientific formulation of land quota distribution policies at the central level carries profound implications for both local economic vitality and national developmental priorities. Nevertheless, inherent information asymmetries in multilevel governance systems [6,7] present policymakers with persistent challenges in accurately assessing heterogeneous regional land demand. This frequently leads to spatial mismatches between allocated quotas and actual developmental requirements, inadvertently constraining local economic potential. Investigating mechanisms for optimizing interregional land

resource allocation thus emerges as a crucial pathway for China to overcome the current economic constraints and achieve sustainable, high-quality development.

This study responds by developing a general equilibrium-based simulation framework for China's territorial spatial planning. Addressing prevalent issues of fragmented, inefficient, and ecologically detrimental land use patterns across China's 31 provincial-level jurisdictions, our model aligns with national quality development objectives and spatial planning policy imperatives. Through a systematic integration of land as an endogenous economic factor within a price-responsive framework, we establish an operational analytical tool that (1) elucidates dynamic interactions between optimal land allocation, socioeconomic progress, and ecological equilibrium; (2) enables precise forecasting of land demand under varied policy scenarios; and (3) mitigates planning inefficiencies arising from suboptimal decision making. The model's dual functionality provides substantive value by supporting central government policymakers with evidence-based spatial strategy formulation while equipping local governments with the technical capacity for informed quota negotiations across administrative boundaries. This dual-level analytical approach ultimately enhances the synergy between national spatial governance objectives and region-specific developmental realities.

2. Literature Review

2.1. The Evolution of China's Land Resource Allocation Patterns

Prior to the reform of China's land resource allocation, land was used without compensation, and resource allocation was entirely planned, leading to inefficiency and constraining socioeconomic development. After the reform and opening-up, the central government developed a mechanism for selecting local officials based on economic growth criteria, which stimulated rapid economic growth but also resulted in uncontrolled land allocation and continuous use of arable land. To address food security and promote sustainable land use, the central government initiated a first round of land use master plans in 1987 [8]. Since then, the concept of indexed land allocation and management has been established. In 1998, the Ministry of Land and Resources was established, and the Land Management Law [9] was amended to require the approval and management of construction, agricultural, and arable land, forming a basic land use control system. This period also saw the initial formation and continuous implementation of China's "top-down" land resource allocation model, the land quota system.

Land quota systems operate through multi-temporal governance frameworks that combine strategic horizons with operational implementation [10]. Structurally, long-term quotas spanning 5–15-year cycles establish binding thresholds for provincial and municipal retention of agricultural land (cultivated, forest, grassland, orchards) and construction land development under national spatial masterplans, forming vertically integrated constraints that guide strategic land use decisions across administrative hierarchies. Operationally, these translate into annual short-term targets governing agricultural land preservation, new construction land supply, and land rehabilitation benchmarks specified in localized implementation plans. The allocation mechanism functions through a dual-track reporting system where subnational governments annually submit land demand projections to superior authorities [11]. These requests undergo rigorous calibration through three evaluative dimensions: compliance verification with masterplan thresholds, contextual adaptation to regional development priorities, and performance monitoring via satellite surveillance systems to deter quota violations, ultimately materializing as district-level allocations for agricultural production zones, infrastructure corridors, and urban expansion limits.

Significantly, our modeling framework, initially conceptualized as a "Land Use Planning Simulation Model", has been reconceptualized in response to China's post-2018 spatial

planning reforms [12]. The transformative multi-plan integration mandate consolidated previously fragmented systems—land use planning, urban–rural development blueprints, and ecological functional zoning—into a unified national territorial space planning framework [13]. This holistic governance model prioritizes development–protection synergies, implements cross-sectoral spatial controls, and governs all-category spatial utilization encompassing ecological, agricultural, and urban domains. Accordingly, our model (CT-SPM) specifically addresses interprovincial allocation dynamics of four critical land types (cultivated land, forest, grassland, construction land) under divergent policy scenarios. The evolution of the nomenclature from "land use planning" to "territorial spatial planning" reflects both institutional restructuring and the model's enhanced capacity to simulate integrated spatial governance outcomes across China's complex administrative landscape.

2.2. Progress in Applied Research on Land Resource Allocation

Initial investigations predominantly employed linear programming frameworks [14–16] to simulate land use patterns through probabilistic distribution forecasts, establishing foundational principles for optimal allocation that remain relevant in contemporary structural analyses. This technique has had a profound impact on the optimal allocation of land uses. There are still scholars [17,18] discussing land use structure issues using linear programming. Despite these seminal contributions, traditional optimization models exhibit inherent limitations in resolving complex spatial configurations. Technological advancements catalyzed a paradigm shift to geographical models based on GIS (Geographic Information System) and RS (Remote Sensing Technology), such as Conversion of Land Use and its Effects (CLUE) [19–21], the Urban Land Use Allocation Model (ULUM) [22], the Integrated Model to Assess the Greenhouse Effect (IMAGE) [23,24], and Future Land Use Simulation (FLUS) [25,26]. Concurrently, the integration of evolutionary computation—notably genetic algorithms [27,28], particle swarm optimization [29], and ant colony systems [30]—enabled multidimensional solutions addressing both quantitative targets and spatial arrangement constraints through micro-level behavioral mechanisms, significantly enhancing decision making relevance. Geographical models and algorithms for simulating land use optimization can make model-based decisions more in line with real-world logic by setting up micro-mechanisms. However, due to the lack of economic mechanisms, they may not be the optimal choice when simulating economic policies. Meanwhile, as a partial-equilibrium model, the linear programming model cannot effectively analyze and predict overall development.

This study advances a Computable General Equilibrium (CGE) framework, selected for its dual analytical merits: (1) robust economic interpretability through integrated sectoral linkages, and (2) multi-scalar adaptability accommodating diverse spatiotemporal resolutions. Grounded in Walrasian general equilibrium theory [31] and operationalized through Johansen's multisectoral growth model [32], CGE frameworks matured into indispensable policy instruments by the late 1970s. Their micro–macro coherence—explicitly connecting agent-level behaviors with macroeconomic outcomes—provides distinct advantages over conventional econometric approaches in simulating complex system interactions. While CGE modeling has been extensively applied in trade economics [33,34], fiscal policy analysis [35,36], and labor migration analysis [37,38], its utilization in land resource allocation remains nascent. Notable examples of land use-related CGE models include the Future Agricultural Resource Model (FARM) [39], the GTAPE-L model [40], the MIRAGE model [41,42], the CGELUC model [43,44], the TERM-BRZ model [45], the TERMCN-Land model [46], and the REGIA model [47].

A critical review of the existing literature reveals that current research on land resource allocation primarily relies on geographical or linear programming models, with a focus on

either the natural or economic attributes of land. Most studies adopt a singular perspective, which does not align with the contemporary multidimensional strategy for national territorial space planning, potentially leading to assessment inaccuracies. Additionally, while the use of multi-regional CGE models for land use simulation is increasing, the majority of research efforts concentrate on agricultural or ecological land, with less attention given to construction land. However, the strategic planning and management of construction land play a crucial role in achieving urban and regional socioeconomic development goals, protecting the environment and enhancing residents' quality of life. Therefore, incorporating the diversity of land uses into the CGE model is essential.

Considering these factors, this paper introduces the China Territorial Spatial Planning Simulation Model (CTSPM), a multi-scale and multi-type model. The CTSPM integrates cultivated, forest, grass, and construction land to simulate the effects of socioeconomic changes and price fluctuations on land use, and to accurately predict land use demands. This model provides a scientific tool for optimizing land resource allocation. Additionally, the inclusion of a land use transition matrix and the revision of the assumption of unlimited land supply enhance the model's realism by specifying the conversion processes between different land types. The addition of a land use demand module for residential and non-agricultural construction land further improves the model's practical applicability.

3. Materials and Methods

3.1. Basic Principle of CTSPM

The CTSPM constructed in this paper distinguishes between 14 industrial sectors (include crops, forestry, livestock, other agriculture, mining, food processing, textiles, wood processing, chemical manufacturing, equipment manufacturing, other manufacturing, water, electricity and gas production and supply, transport services, and other services), 31 provinces and autonomous regions, 2 types of labor force (skilled and unskilled), and 7 types of land use (including arable land, grassland, forested land, rural residential land, construction land, urban residential land, and unutilized land). The model examines changes in the parameters of one or more modules as a result of changes in the parameters of other modules, based on the behavior of economic agents, by establishing links between the modules of the economic system, such as consumption and production. The implementation principle of CTSPM is that the model can be adjusted spontaneously by considering the assumption of the optimal behavior of economic agents, and the model applies a linear expression to depict the linkage between the production side and the demand side. At the same time, the spatial properties of the model are reflected in interregional trade, investment, and labor flows. Following the generally accepted correlation between spatial interactions and general equilibrium models, this paper divides the participants in economic activities into producers and final consumers, with final consumers including the government, residents, domestic and foreign industries. The economic activities are carried out by non-transportation firms, transportation firms, residents, and the government. Meanwhile, production is assumed to involve three factors, namely labor and capital (free-flowing factors) and land (a non-free-flowing factor). Consumption flows, on the other hand, consist of residential consumption, capital investment, and government consumption. It is also assumed that goods can be traded between domestic regions and abroad, and that the quality of goods is the same irrespective of their origin; consumers in different regions have the same preferences for goods. The demand for transport services includes only the demand for the purchase of other goods. All transport costs are paid at the start. Also, because the model is multi-regional, it treats each region as a separate economy, i.e., each region is an individual with the ability to optimize its decision making behavior. The

specific structure of the model is shown in Figure 2, and the main equations of each module are in Appendix A.

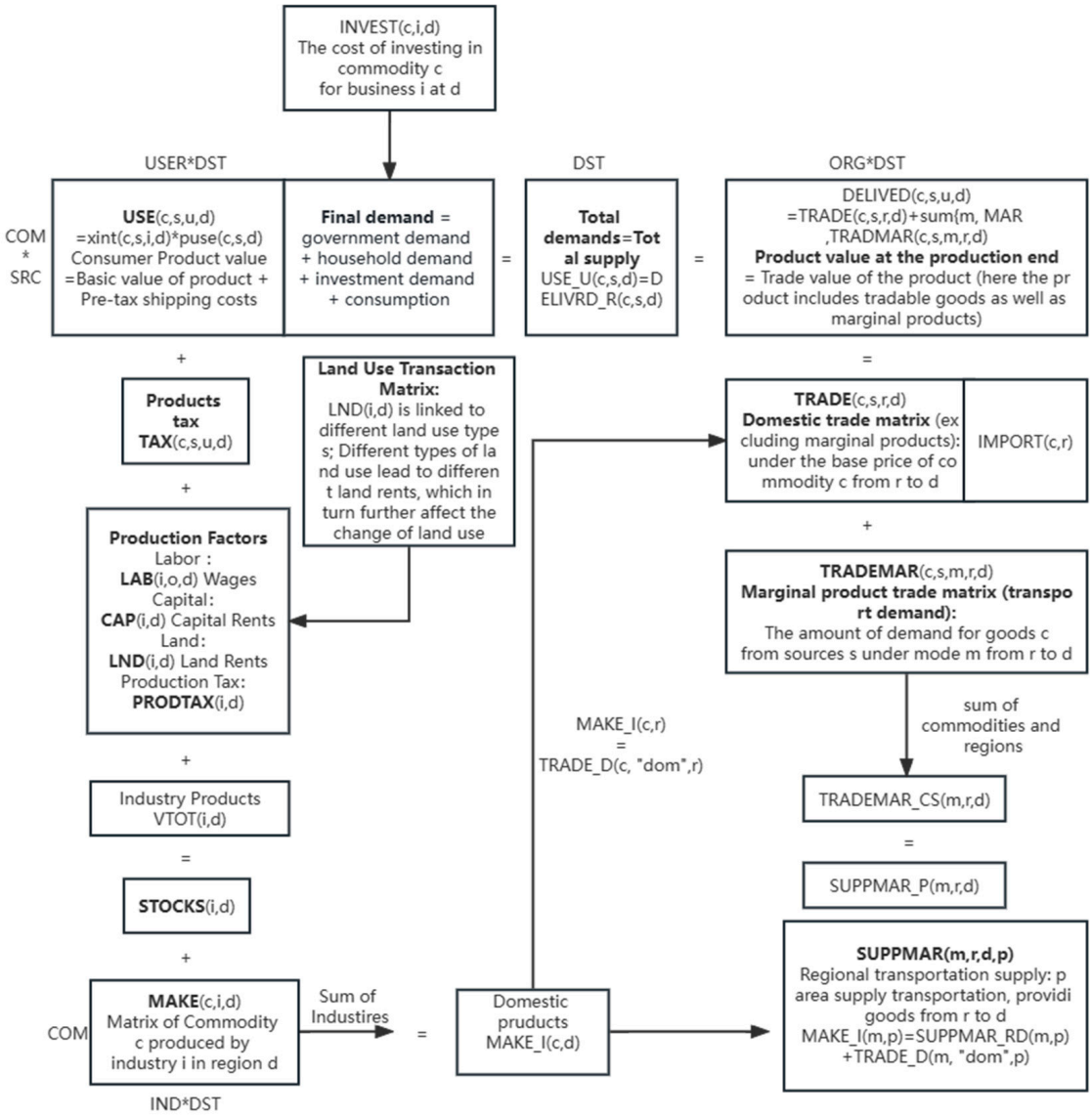

Figure 2. Schematic diagram of CTSPM's structure, where COM*SRC means a matrix with commodities and sources as dimensions; IND*DST means a matrix with industries and regions of use as dimensions; USER*DST means a matrix with users and destinations as dimensions; ORG*DST means a matrix with regions of origin and regions of use as dimensions. Source: Referenced from https://www.copsmodels.com/archivep.htm#tpmh0057 (accessed on 7 October 2004) and modified according to the content of this paper.

3.2. Treatment of the Land Module

The mechanism model of CTSPM is the SinoTERM model, in which the land module is described by adding land as the initial input factor of production in the production function for analysis. However, the SinoTERM model only simulates the land factor from the demand side and the supply of land factor is set to be infinite in the model. The land factor only appears in the agriculture, forestry, livestock, and fishery industries, which use land as an input factor, while secondary and tertiary industry do not consider the input of the land factor. Based on SinoTERM, this paper improves the assumption of an infinite supply of land in the original model by adding the module of land transfer. Through the land demand forecasting module, the use of construction land is also simulated accordingly.

The modeling ideas of the land transfer module and the land demand forecasting module will be introduced later.

Firstly, the model introduces a land use transfer matrix to measure the probability of conversion between agricultural land, forestry land, and livestock land so as to obtain the predicted changes in agricultural land, forestry land, and livestock land for the next time period. The initial land use transition matrix is calibrated to the changes in the shares of the four land uses based on the national 1 km raster data released by the Institute of Geography of the Chinese Academy of Sciences in 2000 and 2010, i.e., Markov probability, which is used to characterize the probability that a specific area of land used for one purpose in two time periods will be used for another purpose in the next time period. The land use transition matrix will be used in the model constructed in this paper to drive the movement of land between uses and thus determine the annual supply of arable land, woodland, and grassland. In the model, the Markov matrix will evolve endogenously in response to changes in the average unit rents of the different sites in each area, and the evolution will follow the following rules:

$$S_{L_1L_2r} = \mu_{L_1r} C_{L_1L_2r} F_{L_2r} P^{\alpha}_{L_2r}, \quad (1)$$

where $S_{L_1L_2r}$ represents the proportion of land type L_1 converted to land type L_2 in region r during the observation period; μ_{L_1r} acts as a slack variable to ensure that $\sum_{L_2} S_{L_1L_2r} = 1$; $C_{L_1L_2r}$ represents the constant term, which acts as a calibration and is set to an initial value of $S_{L_1L_2r}$; $P^{\alpha}_{L_2r}$ denotes the average rental price of land of type L_2; α is a sensitivity parameter with an initial value of 1.25; and F_{L_2r} is a transfer variable with an initial value of 1.

Secondly, considering that the influencing factors are very different for different land types and that the use of multivariate linear fitting has a certain impact on the accuracy of the model due to the limited indicators that can be obtained from the simulation, the prediction of non-agricultural construction land will be carried out by means of classification prediction. For rural residential land, urban residential land, and non-agricultural production land, the gray prediction model and multivariate linear model are used to predict the three types of land, and data from 2000, 2005, 2010, and 2015 are used to fit the three types of land and predict the area of the two types of land in 2020.

Specifically, this paper adopts a gray model approach for the prediction of rural settlement land, looking for patterns in the upward and downward fluctuations in the area of rural settlements so as to predict the future demand for rural residential land. Considering the number of samples and the growing trend of land use changes, this paper uses the gray forecasting model GM(1,1) to simulate the forecast of rural residential land area. The modeling principle is to accumulate the original land use sequence so that the generated sequence has a certain regularity, establish a first-order linear differential equation model to obtain the fitting curve, and then forecast the system. The specific solution process is detailed in Appendix B.

In addition, considering the availability, operability, scientificity, and completeness of the indicators in the measurement of non-agricultural production land and urban residential land, this study starts at the population scale and with economic development. We establish a multiple linear panel regression model based on the relevant data released by the National Bureau of Statistics of each region from 2000 to 2015 in the following formulas:

$$y_1 = \beta_m + \beta_1 x_1 + \beta_2 x_2 \quad (2)$$

$$y_2 = \beta_n + \beta_3 x_3 + \beta_4 x_4, \quad (3)$$

where y_1 is the area of non-agricultural construction land, x_1 is the total population of each province, x_2 is the sum of the value added of the secondary industry and the value added of the transport industry in each province, and β_m is a constant term. Similarly, y_2 is the area of urban residential land, x_3 is the total resident population of the towns and cities in each province, x_4 is the difference between the growth value of the tertiary industry and the value added of the transport industry in each province, and β_n is a constant term.

3.3. Data

Three types of data are used in this paper: macro data on economic development, geographic remote sensing data, and the parameter settings based on the literature and existing information. The economic development macro data, collected from the China Statistical Yearbook [48], China Environmental Statistics Yearbook [49], China Population and Employment Statistics Yearbook [50], China Rural Statistics Yearbook [51], and China Labor Statistics Yearbook [52], are mainly used in subsequent scenario simulation settings. The geographic remote sensing data come from the 1 km land use raster data released by the Institute of Geographic Sciences and Resources of the Chinese Academy of Sciences in 2000 and 2010 [53], and the 30 m land use raster data for the same year are applied to calibrate and supplement the data, which are mainly applied to produce the land use conversion matrix. The parameter setting includes the elasticity parameter values used in the model, which mainly come from the elasticity coefficients of labor wage distribution in the original database of SinoTERM and the GTAP database, and the parameter setting data used in the scenario simulation of the model, which mainly come from the policy documents of land use and economic development prediction and the demand of the development target.

4. Scenario Design

4.1. Basic Scenario

In the basic scenario, we selected GDP growth rate, total factor growth rate, population change, and other related economic development indicators from the two levels of economic development and social progress for the simulation.

From 2020 to 2035, the macroeconomic development is assigned values according to the projection of historical data, with real GDP values available for 2021. The other macroeconomic variables are simulated according to a projection based on historical data. According to the results of the projection, China's real GDP will grow by 31% by 2030, i.e., an average annual growth rate of 2.7%. The reason for the lower level of growth is the economic downturn caused by COVID-19, which led to unsatisfactory GDP growth in China and globally in recent years. The economy began to show signs of a rebound by 2021, with the real GDP growth rate reaching 4.38%. Combined with the IMF's forecast for China's GDP growth in 2022 and the GDP growth target in the 2022 government work report issued by the State Council of China, this paper sets the average GDP growth rate from 2022 to 2035 at 4% in the base period simulation. As for total factor productivity (TFP), it is estimated based on the average value in the past. Based on the historical data, we predict a value of TFP growth of about 1.7% [54].

In making population projections, we referred to the National Population Development Plan (2016–2030) [55] issued by the State Council, the Seventh National Population Census of 2020, and the World Health Organization reports [56] for 2020–2022. We also collected data on China's total population growth, life expectancy, fertility rate, and related demographics, and set the parameters in PADIS-INT software (https://www.cpdrc.org.cn/en/DataandTools/PopulationProjection/202310/t20231014_508.html (accessed on 12 January 2025)) to project the total population from 2022 to 2035. The results show that

China's total population in 2025 will be 1.419 billion, an increase of 0.84% compared to 2020. China's total population in 2030 will be 1.4177 billion—a decrease relative to 2025, but still an overall growth trend with a growth rate of 0.56%—while the total population in 2035 will drop to 1.393 billion, a decline of 1.22%. Considering the long span from 2000 to 2035 and the need for rapid economic growth, a 10% increase in the rate of development of unused land from 2020 to 2035 is set. The specific parameters of the scenario design are shown in Table 1.

Table 1. Parameter settings for basic scenario modeling.

	Scenario Design
Baseline scenario (BASE)	• GDP increase 67.5%; • GDP deflator increase 51.8%; • The total population decrease 1.22%, and the population of labor decrease 6.25%; • TFP increase 28.77%; • Arable land remaining unchanged with an increase of 0%, and a level of unutilized land development of 10%.

4.2. Policy Scenario

High-quality development is characterized by the principles of innovation, coordination, greenness, openness, and sharing, and it aims to meet people's needs for a better quality of life. In this paper, the simulation design for high-quality development scenarios is based on three key aspects: green ecological protection, sustainable development, and scientific and technological progress. The analysis specifically focuses on how scientific and technological advancements impact land demand in provinces and cities, with a particular emphasis on the demand for construction land.

1. Parameter Setting for Green Ecological Protection and Sustainable Development

According to the Master Plan for Major Projects for the Protection and Restoration of National Important Ecosystems (2021–2035), the forest cover rate will increase by 1 percentage point every five years, and by 2035, the forest cover rate will reach 26% [57]. According to our calculation of the forest cover area, in 2020, China's forest cover rate is roughly 23.6%; therefore, we predicted the forest cover rate to reach 26% coverage in 2035. That equates to an increase in forest area of 2.4%.

At the same time, an increase in the population also has an important influence on sustainable economic and social development. The population is the basis of all economic and social activities, and the increase in construction land is directly related to the increase in population. In order to better predict China's future population, we applied PADIS-INT software to predict the population of the whole country, consistent with the base period simulation, and predicted that the total population will decrease by 1.22% by 2035.

For the urbanization rate, it is predicted that China's overall urbanization rate will reach 74% by 2035, which is a 6% increase compared to the urbanization rate in 2020. Therefore, the urbanization rate of each region is taken as the average of the five-year average and the maximum value of 6% to obtain the value of the urbanization rate of each region in the context of high-quality development. Table 2 shows the urbanization rate and urban population of China's provinces and cities in 2035 according to the calculation.

Table 2. Urbanization rate, total population, and urban population in China's 31 provinces in 2035 under policy simulation.

	Urbanization Rate	Population	Urban Population		Urbanization Rate	Population	Urban Population
Beiijng (BJ)	0.91	21.57	1970.06	Hubei (HUB)	0.74	5662.27	4190.05
Tianjin (TJ)	0.94	1367.03	1283.50	Hunan (HUN)	0.70	6549.31	4576.40
Hubei (HB)	0.71	7356.52	5236.74	Guangdong (GD)	0.85	12,442.21	10,608.53
Shanxi (SX)	0.74	3439.74	2532.73	Guangxi (GX)	0.65	4946.73	3230.41
Inner Mongolia (NMG)	0.79	2368.40	1861.77	Hainan (HN)	0.71	997.43	712.03
Liaoning (LN)	0.83	4193.73	3491.72	Chongqing (CQ)	0.81	3162.79	2548.29
Jilin (JL)	0.74	2364.45	1744.05	Sichuan (SC)	0.68	8250.46	5597.24
Heilongjiang (HLJ)	0.77	3125.34	2397.27	Guizhou (GZ)	0.64	3802.44	2443.92
Shanghai (SH)	0.90	2452.17	2213.01	Yunnan (YN)	0.61	4654.00	2846.03
Jiangsu (JS)	0.85	8354.93	7064.58	Tibet (XZ)	0.47	360.73	169.19
Zhejiang (ZJ)	0.83	6374.86	5309.03	Shaanxi (SAX)	0.74	3898.05	2875.39
Anhui (AH)	0.69	6017.09	4178.22	Gansu (GS)	0.63	2464.99	1561.05
Fujian (FJ)	0.80	4101.08	3275.43	Qinghai (QH)	0.71	584.46	415.81
Jiangxi (JX)	0.72	4453.93	3186.50	Ningxia (NX)	0.76	710.62	540.21
Shandong (SD)	0.74	10,018.62	7429.78	Xinjiang (XJ)	0.68	2552.70	1726.52
Henan (HEN)	0.67	9797.85	6519.20				

2. Scientific and Technological Progress

In this paper, total factor productivity (TFP) is selected as an indicator to characterize high-quality economic development. Total Factor Productivity (TFP) measures the quality of a country's economic development. An increase in TFP means that more output can be obtained with the same amount of resource inputs. In this paper, the United States is used as a benchmark country to assign a value of Total Factor Productivity (TFP) (We've chosen the USA as our benchmark country primarily because it stands as a productivity - frontier nation. In the global economic landscape, the USA serves as a standard that most economies aspire to match and progress towards.. China aims to reach the moderately developed country level by 2035. Given the vague definition of such countries (typically between middle-income and highly developed, high-income ones), we, for data availability reasons, deem the USA a developed, high-income nation. The TFP gaps between the USA and East Asian countries such as South Korea and Japan emerged when they became moderately developed. These comparisons helped us to predict China's 2035 TFP target for high-quality development). The logic behind that assignment is as follows. First of all, in the literature [58–61], most scholars predict that China's TFP growth will be between 2% and 3% in the future. It has also been pointed out that, if China is to realize socialist modernization, TFP will need to surpass 2.0%. Secondly, referring to the past experience of developed countries in East Asia such as Japan and South Korea, we can see that their per capita GDP had already reached more than 30% of that of the United States by the 1960s and rose steadily to about 80% of that of the United States in the 1990s. Thereafter, it continued to grow. By observing the changes in their TFP, it can be seen that, around the 1990s, Japan's TFP basically reached 70% of the USA's, and South Korea's was about 65% of the USA's, which, to a certain extent, also proves the role of TFP in economic development. Therefore, this section modeled smooth high-quality development (HQM-S) and rapid high-quality development (HQM-R) scenarios, i.e., scenarios with average annual total

factor productivity growth rates of 2.5% and 2.7%, respectively. As a result, the total factor productivity growth rates by 2035 are predicted to be 44.8% and 49.13%, respectively. The specific parameters of the scenario design are shown in Table 3.

Table 3. Parameter settings for policy scenario modeling.

	Scenario Design
Smooth High-Quality Development Scenario (HQM-S)	• TFP increased by an average of 2.5% per year, with a total increase of 44.8%; • GDP deflator growth of 51.8%; • Forest land increase 2.4%; • Total population decrease 1.22%; • Labor force decrease 6.25%; • The level of unutilized land increase 5%.
Rapid High-Quality Development Scenario (HQM-R)	• TFP increased by an average of 2.7% per year, with a total increase of 49.13%; • GDP deflator growth of 51.8%; • Forest land increase 2.4%; • Total population decrease 1.22%; • Labor force decrease 6.25%; • The level of unutilized land increase 5%.

5. Results

5.1. Changes in National Land Demand Under Different Scenarios

Table 4 shows the changes in national demand for various types of land under the BASE, HQM-S, and HQM-R scenarios. The simulation results show that the area of arable land decreases under the three simulation scenarios, with the smallest decrease in the BASE scenario, by 2.8% from 2020 to 2035, and the largest decrease, by 4.96%, under the HQM-R scenario. The area of green ecological land also shows a decreasing trend under the three scenarios, with the area of grassland showing a decreasing trend across the board. However, the area of forest land shows a decreasing trend under the BASE scenario at 4%, but an increasing trend under the HQM-S and HQM-R scenarios, with an average of 1.8%. The area of non-agricultural construction land grows the fastest under the HQM-R scenario, 31.05%, and the slowest under the BASE scenario, only 25.4%. The area of construction land shows an increasing trend under the three scenarios, reaching 366,298.55 km^2, 370,414.17 km^2, and 373,114.74 km^2 in 2035 under the BASE, HQM-S, and HQM-R scenarios, respectively. The area of urban and rural residential land remained relatively uniform in terms of growth.

According to the data from the Third National Land Survey and the National Land Planning Outline (2016–2030) [62] (hereinafter referred to as "the Outline"), if the condition of arable land holdings determined in the National Land Planning Outline is achieved by 2030, the reduction rate of China's arable land holdings should not be more than 4.8% from 2020 to 2030. If it is assumed that the reduction rate of arable land holdings by 2035 is set at the level of the average annual reduction from 2020 to 2030, then the rate should not be greater than 7%. Based on the simulation carried out in this paper, all of the policies for arable land protection can be accomplished. According to the model for urban and rural construction land, under the base period simulation and different policy scenarios, the area demand for new construction land is 46,281 km^2, 50,396 km^2, and 53,097 km^2, respectively, with reference to the interpretation of land use indexes by the National Development and Reform Commission of the People's Republic of China in the Outline. The average growth of new construction land during the "14th Five-Year Plan" and "15th Five-Year Plan" is 27.6 million mu, and so on; the area of new construction land by 2035 will not exceed

82.8 million mu, i.e., 55,227.6 km^2. From this, it can be judged that the requirements set out in the Outline can be fulfilled under different simulations.

Table 4. Forecasted demand values and rates of change for different land use types in China under base simulation and policy simulation.

Total Land Use Change	Original Data	Baseline Scenario (BASE)	
	Land Use Area (km^2)	Land Use Area (km^2)	Land Use Change
Arable Land	1,775,713.00	1,725,788.04	−2.81
Forest Land	2,228,043.40	2,146,642.05	−3.65
Pasture Land	2,704,259.51	2,411,463.55	−10.83
Green Ecological Land	4,932,302.91	4,558,105.61	−7.59
Non-Agricultural Construction Land	103,246.00	129,511.67	25.44
Urban Residential Land	73,016.00	75,363.60	3.22
Rural Residential Land	143,756.00	161,423.28	12.29
Construction Land	320,018.00	366,298.55	14.46

Total Land Use Change	HQM-S		HQM-R	
	Land Use Area (km^2)	Land Use Change	Land Use Area (km^2)	Land Use Change
Arable Land	1,688,452.25	−4.91	1,687,599.63	−4.96
Forest Land	2,268,164.87	1.80	2,268,164.86	1.80
Pasture Land	2,379,099.11	−12.02	2,379,951.91	−11.99
Green Ecological Land	4,647,263.98	−5.78	4,648,116.76	−5.76
Non-Agricultural Construction Land	132,824.84	28.65	135,303.06	31.05
Urban Residential Land	76,166.05	4.31	76,388.63	4.62
Rural Residential Land	161,423.28	12.29	161,423.28	12.29
Construction Land	370,414.17	15.75	373,114.97	16.59

5.2. Changes in Land Demand by Province in Different Contexts

Figures 3–5 show the changes in the land use structure of different provinces in the eastern, central, western, and northeastern regions from 2020 to 2035 under different scenarios. The results of different policy simulations for the eastern, central, western, and northeastern regions will be interpreted later, and the northeastern region will be merged into the eastern region for ease of analysis when the results are interpreted.

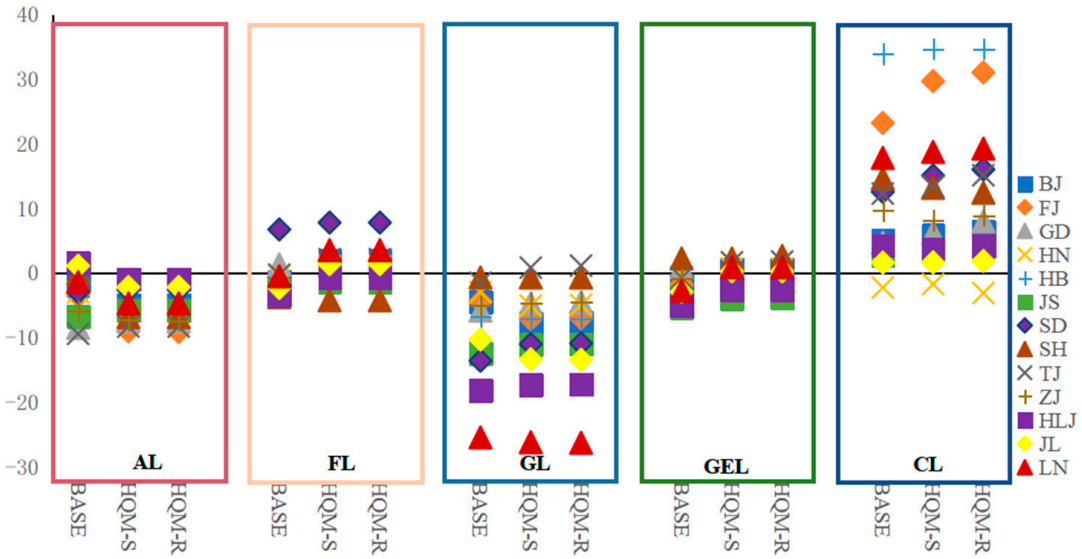

Figure 3. Rates of change in Arable land (AL), Forest Land (FL), Grassland (GL), Green Ecological Land (GEL), and Construction Land (CL) in the eastern and northeastern regions under BASE, HQM-S, and HQM-R. (The legend on the right side corresponds to the abbreviation of the provinces, which can be found in Table 2).

Specifically, the demand for arable land and grassland in the eastern region as a whole shows a decreasing trend, while forest land, green ecological land, and construction land show an increasing trend. As can be seen from the figure, under the BASE scenario, the arable land area of Tianjin decreases most significantly, with a decrease rate of −9.36% by 2035 under the base period simulation, while the arable land of Beijing is the province with the least significant change, with a decrease of only 41 km^2 and a change rate of −1.2%. The change trend of arable land demand under the HQM-S and HQM-R scenarios is basically the same, with the demand for arable land in Shandong province decreasing less (by an average of 2.5%) while the demand for arable land in Zhejiang and Fujian decreases more significantly, by an average of 8% and 7.5%, respectively.

The rate of change in forest land in the eastern region under the BASE scenario is relatively even, in which Shanghai's forest land area decreases the most obviously, with a decrease of 3.5% from 2020 to 2035, while the forest land in Shandong Province shows a clear growth of 573.18 km^2. Under the simulation of the high-quality development policy, Shandong Province shows the most prominent growth of forest land, 7.8%; and the demand for forest land in Shanghai continues to decrease, by 4.2%. Changes in grassland varied significantly under the different scenarios. Specifically, under the BASE scenario, most eastern provinces will go through a grassland demand decrease of 5% or less, while Jiangsu Province and Shandong Province will see the most significant decrease in grassland, more than 10%. Under the high-quality development policy, the demand for grassland in Tianjin shows a positive growth trend, with an average growth rate of 0.8%, while the demand for grassland in other eastern regions continues to shrink, but by a smaller percentage than in the base period simulation, with Jiangsu and Shandong remaining the provinces with the lowest reduction in demand. Overall, the changes in green ecological land use are more concentrated in the different policy simulations, with Shanghai showing the most significant growth in green ecological land use, and Jiangsu and Shandong provinces showing a significant reduction in green ecological land use due to a significant reduction in the area of grassland.

Under the BASE scenario, the demand for construction land in all provinces in the eastern region except Hainan Province shows a clear positive growth trend, with Hebei Province showing the most obvious growth in demand for urban and rural construction land, increasing by 5563 km^2 by 2035, a growth rate of 33%, while Hainan Province is the only province showing a decreasing trend, a −2.2% change. Under the high-quality development policy simulation, the change in demand in the eastern region is similar to the base period simulation, with Hebei Province still showing the highest demand for construction land. Under the high-quality development policy simulation, the trend in demand in the eastern region is similar to that of the BASE scenario, with Hebei Province continuing to have the highest demand for construction land, Fujian Province and Shandong Province showing a more pronounced increase in demand for construction land compared to the BASE scenario, Zhejiang Province showing a decline in demand compared to the BASE scenario, and Hainan Province showing a decline in demand for construction land compared to the BASE scenario. Hainan Province continues to have the lowest demand, with demand for construction land decreasing by 1.67% from 2020 to 2035. As TFP improves further, demand for construction land in Fujian, Shandong, Tianjin, Zhejiang, and Hainan grows further, while Shanghai shows a declining trend.

Hainan Province is the only province that shows negative growth in construction land under the BASE scenario. By analyzing the changes in the industrial structure of the region and the past changes in the demand for land, it can be seen that the growth of urban and rural residential land in Hainan Province is not significant; the urban residential land even showed negative growth between 2005 and 2010. At the same time, the growth rate of

non-agricultural industries in Hainan Province under the BASE scenario is not high, and the proportion of non-agricultural industries is relatively small compared to other provinces in the east and even other regions of the country, so the demand for construction land in Hainan Province will be further reduced in the future. At the same time, the decrease in population by 2035 will lead to a further reduction in the labor force, which will affect the area of land required by industrial enterprises.

In the northeast, there is no significant difference between the different scenarios for arable land and forest land, but it is worth noting the growth of grassland and construction land in the northeast, especially in Liaoning Province. From the figure, it can be seen that the grassland in Liaoning Province has a relatively large shrinkage under both the base period simulation and the policy simulation, of nearly 30%, which is the largest shrinkage of grassland in the whole country. According to the data on the output value of animal husbandry and the area of grassland in Liaoning Province in recent years, it can be seen that the output value of animal husbandry contributes prominently to the total GDP of the province. The reduction in demand for grassland does not affect the output value of animal husbandry to the total GDP, but also does not affect the growth in grassland. The reduction in grassland demand does not affect the contribution of livestock production value to GDP, so it can be judged that the livestock industry in Liaoning Province is more dependent on TFP.

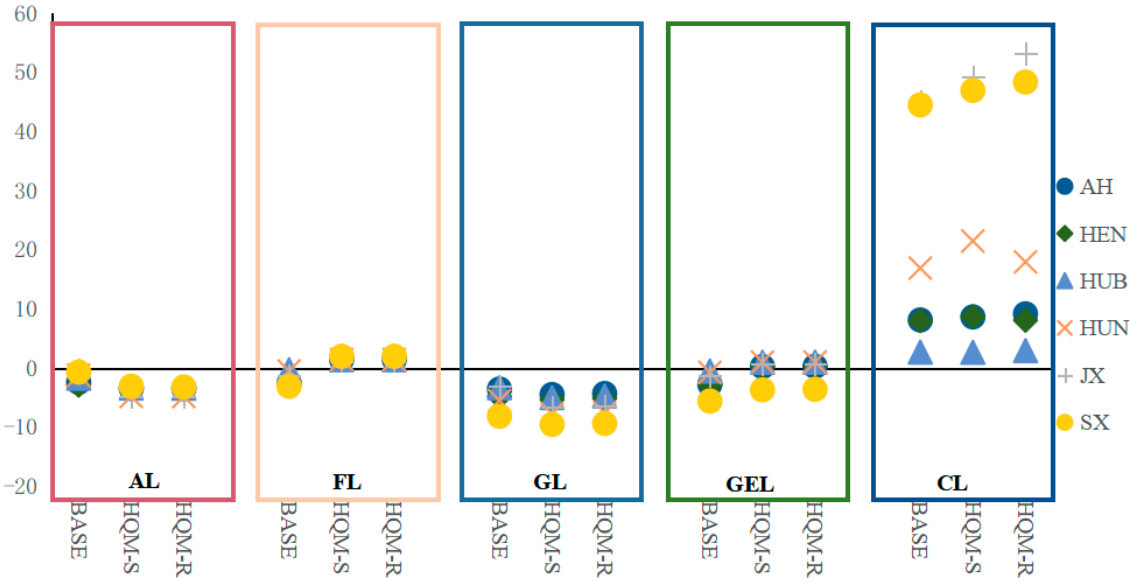

Figure 4. Rates of change in Arable land (AL), Forest Land (FL), Grassland (GL), Green Ecological Land (GEL), and Construction Land (CL) in the central regions under BASE, HQM-S, and HQM-R.

In the central region, the changes in area of arable land and forest land are more even, and the shrinkage of grassland in Shanxi Province is more obvious, which also causes the overall shrinkage of green ecological land in Shanxi Province. Changes in construction land in the central region are more obvious, as can be seen from Figure 2. With the growth in TFP, the area of construction land in Jiangxi Province rises further, reaching the maximum value of construction land demand under the HQM-R scenario, a 53.1% increase in demand. Compared with the scenario of the increase in total factor productivity, the demand for total construction land in Hunan Province also grows correspondingly.

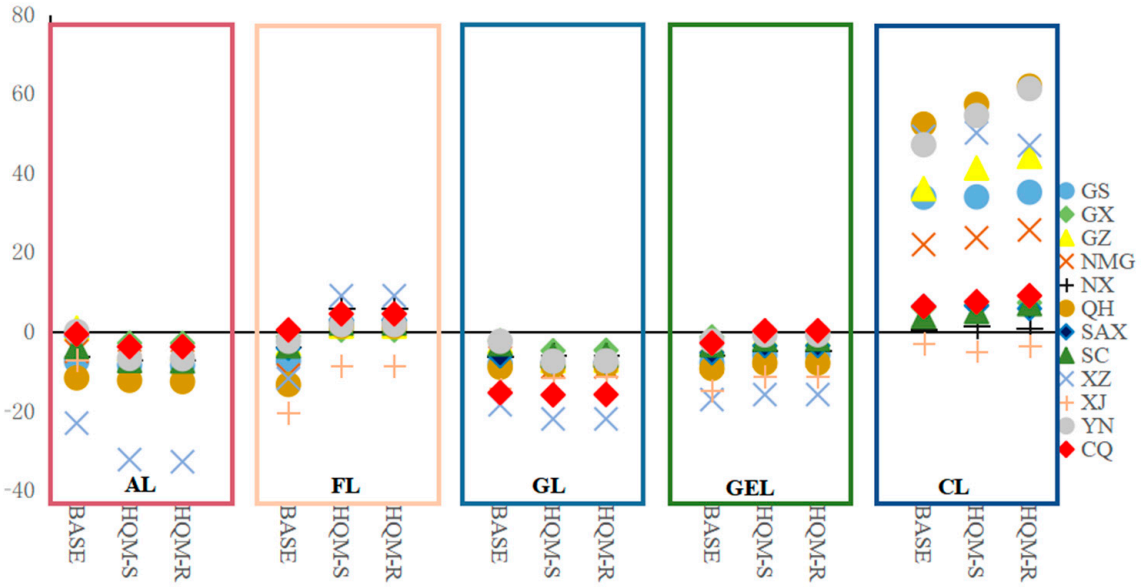

Figure 5. Rates of change in Arable land (AL), Forest Land (FL), Grassland (GL), Green Ecological Land (GEL), and Construction Land (CL) in the western regions under BASE, HQM-S, and HQM-R.

The difference in land use demand in the western region is more obvious, specifically. Arable land area in Tibet has been showing a shrinking trend, and under the HQM-R simulation, the shrinkage is most obvious, with a reduction rate of 32.8%, and the cultivated land area in Chongqing and Yunnan provinces has the least change, with an average change rate of −1.5%. Under the BASE scenario, the forested land in the western region shows a decreasing trend, and the forested land in Xinjiang has the most obvious decrease. Under the policy simulation, the forested land in each region has rebounded, but the forested land in Xinjiang region is still in a negative growth state. The decline in grass land in Tibet is also relatively obvious, although the shrinkage of livestock in Tibet has recovered under the simulation scenario of HQM-R, but the average shrinkage rate also reaches 22%. The demand for construction land in different provinces in the western region varies significantly, with the demand for construction land in Chongqing and Guangxi show an upward trend from the BASE scenario to the HQM-R simulation, and the demand for construction land in Guizhou, Yunnan, Gansu, Qinghai, and Xinjiang continuing to rise from the base period simulation to the HQM-R simulation. The demand for construction land in Tibet is the highest under HQM-S, while the demand for construction land is the lowest under HQM-R.

5.3. Changes in Economic and Social Indicators Under Different Scenarios

From Table 5, it can be seen that the real GDP will grow to RMB 1,771,434.64 billion, RMB 1,964,547.46 billion, and RMB 2,094,946.20 billion under the BASE, HQM-S, and HQM-R scenarios, respectively. The level of economic growth in the policy simulation scenarios is greater than that of the BASE scenario, with the real GDP under the HQM-R scenario growing the fastest—by 98.09% compared to 2020, an average annual growth rate of 4.66%. The BASE scenario shows the smallest increase in CPI, with an average annual CPI increase of 2.7%. Assuming that the RMB will rise by 7% against the USD in 2035 (i.e., the exchange rate will change to 6.35) and considering that the inflation rate will return to normal in the long term after the USA raises interest rates—i.e., assuming that the inflation rate in the USA will increase by 2% per annul during the 15-year period—then it can be calculated that the real GDP per capita will be more than USD 20,000 in 2035 under the policy simulation. Under the HQM-R scenario, real GDP per capita peaks at USD

23,138, while in the BASE scenario, real GDP per capita is below USD 20,000, implying that real GDP per capita nearly doubles over the 15-year period. Conservatively, inflation in the United States is forecasted to increase by 1%, which means that China's per capita GDP will be close to USD 25,000 per capita under the policy simulation, far exceeding the threshold for high-income countries. China will be able to achieve the Vision 2035 goals under the policies of green, innovative, and sustainable development. Moreover, China's current economic development strategy, which focuses on expanding domestic demand, has proven to be highly effective. Through the simulations of our model, we found that, in the HQM-R scenario, characterized by rapid TFP growth, both household consumption and total capital formation will experience substantial increases. The model predicts that, by 2035, these two indicators will rise by 96.2% and 55.1%, respectively, fully validating the multiplier effect of an innovation-driven development strategy on consumption upgrading and investment optimization. Notably, there are significant differences in the international trade landscape under different development paths: in the baseline scenario, imports and exports maintain balanced development. However, in the two TFP-enhanced scenarios, the growth rate of exports outpaces that of imports, creating a noticeable divergence. This gap widens as TFP growth increases. This structural change suggests that policymakers need to establish a dynamic balancing mechanism. While advancing supply-side structural reforms, they should also improve policies to promote imports and guard against the risks of international payment imbalances that may arise from excessive trade surpluses, thereby ensuring the sustainability of coordinated development between domestic and foreign demand.

Table 5. The overall macroeconomic changes in China under the BASE, HQM-S, and HQM-R scenarios in 2035.

%	BASE	HQM-S	HQM-R
Real household expenditure	68.26	84.65	96.21
Real investment	48.1	49.28	55.13
Real government expenditure	70.08	86.64	98.29
export	140.2	175.57	193.95
import	138.37	135.73	139.31
Real GDP	67.5	85.76	98.09
CPI	51.09	52.78	53.39
Population	−1.22	−1.22	−1.22
Nominal GDP	138.76	162.22	177.76
	BASE	**HQM-S**	**HQM-R**
Real GDP (Billions Yuan)	1,771,434.64	1,964,547.46	2,094,946.20
Population (Millions people)	1392.9264	1392.9264	1392.9264
GDP per capita (Yuan/person)	127,173.60	141,037.42	150,398.92

Overall, as is evident from Figure 6, under the BASE scenario and policy simulations, the eastern region contributes more significantly to national GDP growth, while the western region contributes less. In terms of different regions, under the BASE scenario, the real GDP growth of Beijing, Fujian, and Shanghai is most obvious, with real GDP growing by 81%, 80.7%, and 79.9%, respectively, from 2020 to 2035, while the real GDP growth rates of Guizhou, Inner Mongolia, and Ningxia are the least changed at 52.8%, 51.5% and 49.5%, respectively. Under the HQM-S, the real GDP growth of Shanghai is the most obvious. In the factor productivity improvement policy simulation, Shanghai, Guangdong, and Fujian are the most responsive to the policy, with average real GDP growth rates of 103%, 102%, and 100% from 2020 to 2035. Under the HQM-R scenario, the growth rate of real GDP increases further. The average real GDP growth rate is close to 120% (117.8%, 115.7%, and 114.2%, respectively), while Guizhou, Inner Mongolia, and Ningxia remain the regions with the weakest response to the policy.

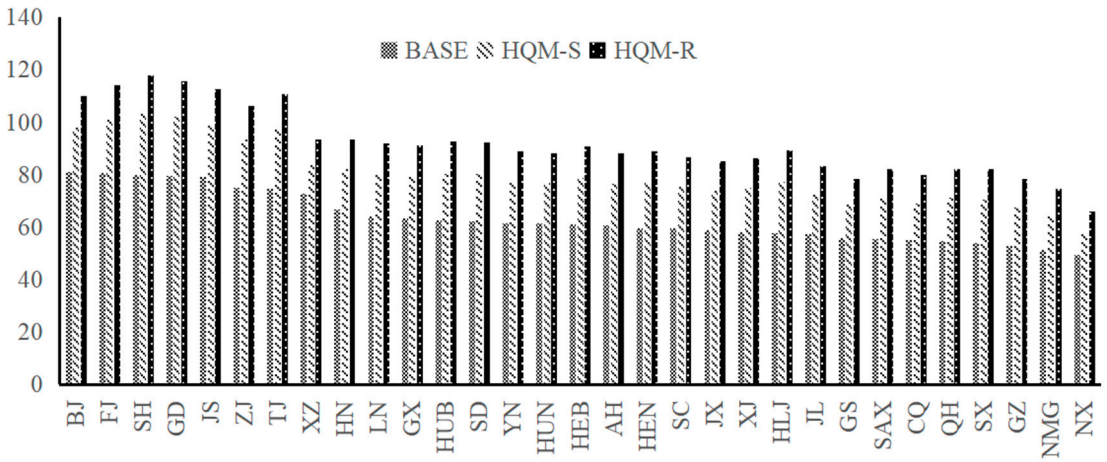

Figure 6. The change rate of GDP of each province in 2035 under the BASE, HQM-S, and HQM-R scenarios.

From the analyses, it can be seen that Shanghai, Fujian, Guangdong, Jiangsu, and Beijing are more responsive to the policy, which is also related to the fact that these provinces and cities have better economies of their own and thus will experience faster GDP growth rates under the high-quality development scenario. It is worth noting that the rate of change in GDP in Tibet has been more pronounced under both the base period simulation and the high-quality development simulation. Between 2020 and 2035, the growth rate of real GDP in the Tibetan region is predicted to be relatively high. This may be due to the rapid development of the Tibetan region in recent years. According to data published by the National Bureau of Statistics, from 2000 to 2020, the average real GDP growth rate of Tibet was 3.2%, which ranks highly among the average real GDP growth rates of all provinces and cities. In the last two years, the average real GDP growth rate of Tibet reached 4%, ranking first. The rapid development of Tibet's GDP can be explained by the fact that the total factor productivity in the setup has increased more than the current level of Tibet itself, and there are technology spillovers.

5.4. Model Robustness Analysis

As the simulation in this paper involves macroeconomic changes and changes in land use, especially construction land use, and changes in construction land use are related to the GDP of non-agricultural industries, as well as the simulation of arable land and green ecological land use, the production function is crucial in this paper. Therefore, in the robustness analysis of the model, taking the historical projection scenario as an example, the parameter variation of the production function is increased or decreased by 10% and 5% to observe the error variation of the real GDP of the region. The upper and lower limits of the confidence intervals are the permissible error ranges. As can be seen from Table 6, the error of real GDP of each province is within the 95% confidence interval, thus indicating that the model is relatively robust in the simulation.

Table 6. Mean of errors and confidence intervals of real GDP of Chinese provinces in the robust test.

Real GDP	Mean of Errors	Lower Level of Confidence Interval	Upper Level of Confidence Interval
Beiijng (BJ)	−0.0178	−2.18	2.18
Tianjin (TJ)	−0.0199	−2.77	2.77
Hubei (HB)	0.00448	−0.283	0.283
Shanxi (SX)	0.0117	−1.47	1.47
Inner Mongolia (NMG)	0.0149	−1.51	1.51
Liaoning (LN)	0.00256	−0.022	0.022

Table 6. *Cont.*

Real GDP	Mean of Errors	Lower Level of Confidence Interval	Upper Level of Confidence Interval
Jilin (JL)	0.00692	−0.51	0.51
Heilongjiang (HLJ)	−0.000786	−2.39	2.39
Shanghai (SH)	−0.0129	−2.46	2.46
Jiangsu (JS)	−0.00255	−0.994	0.994
Zhejiang (ZJ)	−0.00286	−0.0641	0.0641
Anhui (AH)	0.0063	−1.56	1.56
Fujian (FJ)	−0.00136	−0.248	0.248
Jiangxi (JX)	0.00367	−1.66	1.66
Shandong (SD)	0.00593	−0.124	0.124
Henan (HEN)	0.00662	−1.19	1.19
Hubei (HUB)	0.000244	−0.404	0.404
Hunan (HUN)	0.00312	−0.624	0.624
Guangdong (GD)	−0.00982	−1.59	1.59
Guangxi (GX)	0.00349	−1.3	1.3
Hainan (HN)	0.0111	−0.481	0.481
Chongqing (CQ)	0.00513	−0.987	0.987
Sichuan (SC)	0.00419	−1.13	1.13
Guizhou (GZ)	0.0119	−1.85	1.85
Yunnan (YN)	0.0058	−1.1	1.1
Tibet (XZ)	0.00888	−4.42	4.42
Shaanxi (SAX)	0.00384	−0.743	0.743
Gansu (GS)	0.00785	−1.16	1.16
Qinghai (QH)	−0.000711	−0.257	0.257
Ningxia (NX)	0.013	−2.27	2.27
Xinjiang (XJ)	0.00243	−0.436	0.436

6. Discussion

Current research on high-quality development and land use changes often focuses on their interrelationship. Yang et al. [63] found that changes in land functions in China directly shape regional economic development, noting that urbanization can both enhance efficiency and cause environmental issues. Chen et al. [64] showed that water-saving and intensive land use in the Yellow River Basin boost agricultural productivity. Keola et al. [65] linked land characteristics to economic growth using global data, while Yu et al. [66] developed a "land cover efficiency" framework to analyze decoupling in Chinese urban areas. Although existing studies have explored the relationship between land use changes and economic development from multiple angles, they often rely on historical data to uncover quantitative patterns, with limited consideration of policy implications. The CGE model is able to incorporate the behavior of the economic system in response to external stimuli into its analytical system, decompose the economy into different sectors, take into account the interrelationships between sectors and commodities in terms of production and demand, and set up the production function and the land utility function on the basis of macro- and micro-economic theories. This framework is supported by economic theories and is more closely aligned with real economic and social functioning [67]. In recent years, some scholars have considered introducing the concept into economic theory, specifically the analysis and forecasting of land resources. For example, coupled CGELUC and DLS models were used to predict land use patterns in Shandong Province from 2015 to 2025 [68]. Additionally, CGE models with utility functions were constructed to analyze land structure changes in Yunnan [69] and Jiangxi Provinces [70]. However, these studies generally focus on traditional land use patterns and overlook the constraints imposed by high-quality development policies, limiting their practical significance for macroeconomic decision making in the context of China's socioeconomic system transformation. Moreover, existing research often focuses on changes in farmland or forest land under different policies, with less attention paid to the integration of construction land, a key driver of China's economic development, into CGE models. Building on this, our study makes improvements and innovations. In terms of the model specification, we incorporated land resources as a

production factor in various industries, reflecting the heterogeneity of land use across sectors. In the analytical framework, we integrated China's multidimensional high-quality development policies with a land use CGE model to forecast the land use structures of Chinese provinces by 2035 under different high-quality development scenarios. This enhances the application of the land use CGE model in addressing economic development issues and provides feasible solutions for China's land resource management.

Overall, our CGE model results are consistent with those of other studies using similar methods. For example, Song and Jin [71], using Hubei Province as a case study, applied a CGE model to predict the land use structures of the primary, secondary, and tertiary sectors under shared socioeconomic pathways. Their findings indicated a close relationship between TFP and construction land changes, with higher TFP growth rates leading to increased construction land and reduced farmland. The increase in construction land ranged from 5% to 30%, depending on the scenario settings. However, there are some limitations to the CGE model used in this study. First, as a national macroeconomic model, it only considers the quantity and structure of land use, without addressing spatial optimization. Second, the land module, particularly the construction land demand module, could be further refined to better reflect price relationships. We introduced a land use transition module to endogenously regulate farmland and green ecological land, while the prediction of construction land demand was derived through simultaneous equations of output and population. The industrial output is endogenously determined within the model, allowing for a degree of market-based allocation of construction land. The reason for not fully implementing a market-based design for construction land is the difficulty of obtaining rental data for industrial land in different regions. Finally, CGE models require many parameters (such as elasticities) supported by empirical evidence, which is often insufficient [72]. A common method for determining these exogenous parameters is to use data from existing studies, as we did in this research. However, inconsistencies may arise across regions and time periods.

In future work, considering the importance of spatial optimization for land resource allocation, we plan to use geographic models such as CLUE to project optimized land use quantities and structures spatially and conduct in-depth research on the spatial optimization of land use. Additionally, if we can obtain more comprehensive data on construction land prices in different regions, we will be able to design a more accurate land factor market.

7. Conclusions and Policy Implications

7.1. Conclusions

China is currently in a critical phase of national spatial land planning, with the new round of planning focusing on the rational allocation of land resources and the coordinated development of human–land relations. Given the current issues in land use allocation and the tension between land development and protection, this paper constructs a simulation model to predict future land demand and simulate the impact of high-quality development. The main conclusions are as follows:

(1) Both smooth and rapid high-quality development scenarios will significantly boost the economic growth of the entire country, as well as that of individual provinces and cities. Under these two scenarios, the national per capita GDP is projected to double by 2035. The eastern region, in particular, shows a faster increase in GDP contribution as total factor productivity (TFP) rises, while the western region, especially the northwestern part, exhibits slower growth in GDP contribution despite TFP increases.

(2) In line with the land use constraints from the National Land Planning Outline (2016–2030), our high-quality development policy simulations show that arable land will decrease but within the limits set by the Outline; forest land will show a positive

trend, though not meeting the expected growth rate; grassland will reduce to some extent; and construction land, particularly non-agricultural construction land, will see significant growth, while urban residential areas will grow more moderately. The eastern region has a higher demand for construction land, driven by its substantial increase in output value, whereas in the western region, construction land demand varies significantly across different areas.

7.2. Policy Implications

To address the complex interactions between land resource allocation, regional disparities, and sustainable development, we propose the following two policy recommendations based on the findings of this study:

(1) Implement a Differentiated Spatial Governance Framework:

To address regional development imbalances, we propose a multilevel flexible indicator system. This includes a dynamic adjustment mechanism at national, regional, and provincial levels. For eastern urban clusters with high construction land demand, a cross-regional trading market should be established using provincial land quotas to optimize resource allocation. Western regions, like Northwest China, should obtain flexible construction land quotas and infrastructure investments to boost productivity and address the lag in GDP response to TFP. In provincial planning, we suggest increasing the allocation weight for construction land in eastern regions by 15–20% and raising the protection weight for ecological land in western regions by 10%.

(2) Establish a Planning Implementation Assurance System:

To ensure the effectiveness of policy implementation, we propose a three-pronged assurance mechanism. First is to set aside 10–15% of strategic buffer zones in national spatial planning, managed under a "total quantity locked, flexible layout" model. Second is to develop a monitoring and evaluation system with core indicators, generating quarterly reports on the health of the national spatial environment. Third is to enhance the legal support system by revising the provisions in the Implementation Regulations of the Land Management Law related to indicator adjustments. This would clarify the procedures for emergency adjustments in cases where GDP growth fluctuates by more than ± 1.5 percentage points or in the event of major natural disasters.

This dual approach transforms land governance into a responsive, region-specific, and equity-oriented system, ensuring that the vision of high-quality development is more than just rhetoric and reshapes China's spatial future.

Author Contributions: Conceptualization, L.W. and T.S.; methodology, L.W.; software, L.W.; validation, L.W. and Y.H.; formal analysis, L.W.; investigation, L.W.; resources, L.W.; data curation, L.W.; writing—original draft preparation, L.W.; writing—review and editing, L.W. and Y.H.; visualization, L.W.; supervision, T.S.; project administration, T.S.; funding acquisition, T.S. All authors have read and agreed to the published version of the manuscript.

Funding: This research was funded by the Major Program of Beijing Social Science Fund, grant number 24JCA003.

Data Availability Statement: The original contributions presented in this study are included in the article. Further inquiries can be directed to the corresponding author.

Conflicts of Interest: The authors declare no conflict of interest.

Appendix A

The CTSPM consists of five modules: production behavior module, consumption behavior module, government and investment behavior module, trade module and regional supply and demand equilibrium module. Each module is equipped with corresponding equations of supply relationship, demand relationship and equilibrium relationship between the two. The main equations of the different modules will be given in the subsequent section. Since the model constructed in this paper involves multiple regions, multiple labor forces and multiple types of commodities, most of the variables are mostly combinations of multiple dimensions. The set of commodities is denoted by COM and the abbreviation c is used to denote the commodity dimension; the marginal product is denoted by MAR and the abbreviation m is used to denote the marginal product dimension; DST, ORG, and PRD denote the place of use, the place of origin, and the place of production of the produced commodities, respectively, and the abbreviations d, r, and p are used to denote the dimensions of the place of use, the place of origin, and the place of production of the commodities, respectively; IND is the producer and is denoted by i for the producer dimension; SRC for the source of the commodity, including the domestic dimension and the import dimension, denoted by dom and imp; OCC for the type of labor force, denoted by o in equations.

Production Behavior Module:

$$\mathrm{LAB}_{\mathrm{O(i,d)}} = \left(\frac{\mathrm{PLAB}_{\mathrm{O(i,o,d)}} * \mathrm{ALAB}_{\mathrm{O(i,o,d)}}}{\mathrm{PPRIM}_{\mathrm{(i,d)}}}\right)^{-\sigma_{\mathrm{PRIME}}} * \mathrm{XPRIM}_{\mathrm{(i,d)}} * \mathrm{ALAB\_O}_{\mathrm{(i,d)}} \quad \text{(A1)}$$

$$\mathrm{CAP}_{\mathrm{(i,d)}} = \left(\frac{\mathrm{PCAP}_{\mathrm{(i,o,d)}} * \mathrm{ACAP}_{\mathrm{(i,o,d)}}}{\mathrm{PPRIM}_{\mathrm{(i,d)}}}\right)^{-\sigma_{\mathrm{PRIME}}} * \mathrm{XPRIM}_{\mathrm{(i,d)}} * \mathrm{ACAP}_{\mathrm{(i,d)}} \quad \text{(A2)}$$

$$\mathrm{LAND}_{\mathrm{(i,d)}} = \left(\frac{\mathrm{PLAND}_{\mathrm{(i,o,d)}} * \mathrm{ALAND}_{\mathrm{(i,o,d)}}}{\mathrm{PPRIM}_{\mathrm{(i,d)}}}\right)^{-\sigma_{\mathrm{PRIME}}} * \mathrm{XPRIM}_{\mathrm{(i,d)}} * \mathrm{ALAND}_{\mathrm{(i,d)}} \quad \text{(A3)}$$

$$\mathrm{XPRIM}_{\mathrm{(i,d)}} = \mathrm{XTOT}_{\mathrm{(i,d)}} * \mathrm{ATOT}_{\mathrm{(i,d)}} * \mathrm{APRIM}_{\mathrm{(i,d)}} \quad \text{(A4)}$$

$$\mathrm{XINT}_{\mathrm{S(c,i,d)}} = \mathrm{ATOT}_{\mathrm{(i,d)}} * \mathrm{AINT}_{\mathrm{S(c,i,d)}} * \mathrm{XTOT}_{\mathrm{(i,d)}} * \left(\frac{\mathrm{PPUR}_{\mathrm{S(c,i,d)}} * \mathrm{AINT}_{\mathrm{S(c,i,d)}}}{\mathrm{PINT}_{\mathrm{(i,d)}}}\right)^{-0.15} \quad \text{(A5)}$$

Consumption Behavior Module:

$$\mathrm{XHOU}_{\mathrm{(c,s,d)}} = \mathrm{XHOU\_S}_{\mathrm{(c,d)}} * \left(\frac{\mathrm{PPUR}_{\mathrm{(c,s,“HOU”,d)}}}{\mathrm{PHOU}_{\mathrm{(c,d)}}}\right)^{-\mathrm{SIGMADOMIMP}_{\mathrm{(c)}}} \quad \text{(A6)}$$

$$\mathrm{WHOUTOT}_{\mathrm{(d,h)}} = \mathrm{PHOUTOT}_{\mathrm{(d,h)}} * \mathrm{XHOUTOT}_{\mathrm{(d,h)}} \quad \text{(A7)}$$

$$\mathrm{XHOUTOT}_{\mathrm{(d,h)}} = \sum_{\mathrm{c}\in\mathrm{COM}} \mathrm{BUDGSHR}_{\mathrm{(c,d,h)}} * \mathrm{XHOUH\_S}_{\mathrm{(c,d)}} \quad \text{(A8)}$$

$$\mathrm{PHOUTOT}_{\mathrm{(d,h)}} = \sum_{\mathrm{c}\in\mathrm{COM}} \mathrm{BUDGSHR}_{\mathrm{(c,d,h)}} * \mathrm{PHOU}_{\mathrm{(c,d)}} \quad \text{(A9)}$$

$$\mathrm{XHOUH\_S}_{\mathrm{(c,d)}} = \mathrm{XLUX}_{\mathrm{(c,d,h)}}^{\mathrm{BLUX}_{\mathrm{(c,d,h)}}} * \mathrm{XSUB}_{\mathrm{(c,d,h)}}^{(1-\mathrm{BLUX}_{\mathrm{(c,d,h)}})} \quad \text{(A10)}$$

Government and Investment Behavior Module:

$$\mathrm{XGOV}_{\mathrm{c,s,d}} = \mathrm{FGOVTOT}_{\mathrm{d}} + \mathrm{FGOV}_{\mathrm{c,s,d}} + \mathrm{FGOV\_S}_{\mathrm{(c,d)}} \quad \text{(A11)}$$

$$\mathrm{XINVI}_{\mathrm{(c,s,d)}} = \mathrm{XINV\_S}_{\mathrm{(c,d)}} * \left(\frac{\mathrm{PPUR}_{\mathrm{(c,s,“INV”,d)}}}{\mathrm{PINVEST}_{\mathrm{(c,d)}}}\right)^{-\mathrm{SIGMADOMIMP}_{\mathrm{(c)}}} \quad \text{(A12)}$$

$$\mathrm{XINVI}_{(c,i,d)} = \mathrm{RATIO}_{(c,i,d)} * \mathrm{XINVITOT}_{(i,d)} \tag{A13}$$

$$\mathrm{XINVITOT}_{(i,d)} = \mathrm{GGRO}_{(i,d)} * \mathrm{XCAP}_{(i,d)} \tag{A14}$$

$$\mathrm{GGRO}_{(i,d)} = \mathrm{FINV1}_{(i,d)} * \left(\frac{\mathrm{GRET}_{(i,d)}{}^{2}}{\mathrm{INVSLACK}}\right)^{0.33} \tag{A15}$$

$$\mathrm{GRET}_{(i,d)} = \frac{\mathrm{PCAP}_{(i,d)}}{\mathrm{PINVITOT}_{(i,d)}} \tag{A16}$$

Trade Module:

$$\begin{aligned}\mathrm{XSUPPMAR}_{(m2,r,d,p)} &= \mathrm{XSUPPMAR}_{P(m2,r,d)} * \mathrm{ASUPPMAR}_{(m2,r,d,p)}{}^{(1-\mathrm{SIGMAMAR(m)})} \\ &* \left(\frac{\mathrm{PDOM}_{(m2,p)}}{\mathrm{PSUPPMAR}_{P(m2,r,d)}}\right)^{-\mathrm{SIGMAMAR(m)}}\end{aligned} \tag{A17}$$

$$\mathrm{XTRADMAR}_{(c,\text{“dom”},m,r,d)} = \mathrm{XTRAD}_{(c,\text{“dom”},r,d)} + \mathrm{ATRADMAR}_{(c,\text{“dom”},m,r,d)} \tag{A18}$$

$$\mathrm{TRADMAR}_{(c,\text{“dom”},m,r,d)} = \mathrm{XTRADMAR}_{(c,\text{“dom”},m,r,d)} * \mathrm{PSUPPMAR\_P}_{(m,r,d)} \tag{A19}$$

$$\mathrm{TRADE}_{(c,\text{“dom”},r,d)} = \mathrm{XTRAD}_{(c,\text{“dom”},r,d)} * \mathrm{PBASIC}_{(c,\text{“dom”},r)} \tag{A20}$$

$$\mathrm{PPUR\_S}_{(c,u,d)} = \sum_{s\in(\mathrm{dom,imp})} \frac{\mathrm{PUR}_{(c,s,u,d)}}{\mathrm{PUR\_S}_{(c,u,d)}} \mathrm{PPUR}_{(c,s,u,d)} \tag{A21}$$

$$\mathrm{PUR}_{(c,s,u,d)} = \sum_{u\in\mathrm{USR}} \mathrm{PPUR}_{(c,s,u,d)} * \mathrm{XUSR}_{(c,s,u,d)} \tag{A22}$$

$$\mathrm{XEXP}_{(c,s,d)} = \mathrm{FQEXP}_{(c,s)} * \mathrm{FQEXP}_{CS} * \left(\frac{\mathrm{PPUR}_{(c,s,EXP,d)}}{\mathrm{FQEXP}_{(c,s)} * \mathrm{PHI}}\right)^{-|\mathrm{EXP_{ELAST}}|} \tag{A23}$$

Appendix B

In this paper, the gray model forecasting method is used for the forecasting of rural settlements to find patterns in the upward and downward fluctuations of the area of rural settlements, so as to forecast the future demand for rural residential land. The gray model is suitable for the prediction of small sample data, requires less modeling information, and has higher simulation accuracy for non-linear, especially exponential growth trends, which makes it an effective tool to deal with the prediction of small samples. Considering the number of samples and the growth trend in land use change, this paper adopts the gray prediction model GM(1, 1) to simulate and predict the land use of rural settlements. The modeling principle is to make cumulative generation of the original land use sequence, so that the generated sequence is a certain regularity, and then establish a first-order linear differential equation model to obtain the fitted curve to predict the system, and its solution process is as follows:

The original land use sequences are first given for each year:

$$X^{(0)} = \left\{x^{(0)}(1), \ldots, x^{(0)}(n)\right\} \tag{A24}$$

The original land use cumulative sequences can be obtained by summing the sequences:

$$\mathrm{X}^{(1)} = \left\{\mathrm{x}^{(1)}(1), \ldots, \mathrm{x}^{(1)}(\mathrm{k})\right\} \tag{A25}$$

where $\mathrm{x}^{(1)}(\mathrm{k}) = \sum_{\mathrm{m}=1}^{\mathrm{k}} \mathrm{x}^{(0)}(\mathrm{m})$,$\mathrm{k} = 2, \ldots, \mathrm{n}$

The gray differential equation is structured as follow:

$$\mathrm{x}^{(0)}(\mathrm{k}) + \mathrm{az}^{(1)}(\mathrm{k}) = \mathrm{b} \tag{A26}$$

where $x^{(0)}(k)$ represents the residential land area in year k, a represents the evolution parameter, b represents the gray action quantity. $z^{(1)}(k)$ as a sequence of immediate neighboring means of $x^{(1)}(k)$, which is solved as follows:

$$Z^{(1)} = \frac{1}{2}x^{(1)}(k) + \frac{1}{2}x^{(1)}(k-1) \tag{A27}$$

For the gray differential equation, by considering the moments of $x^{(0)}(k)$ as continuous, the primary differential equation with respect to time t is obtained, which is the whitened differential equation of the gray differential equation in the form of the following equation:

$$\frac{dx^{(1)}(k)}{dt} + ax^{(1)}(k) = b \tag{A28}$$

The resulting solution of $x^{(1)}(t)$ is:

$$x^{(1)}(t) = \left(x^{(0)}(1) - \frac{b}{a}\right)e^{-ak} + \frac{b}{a}, k = 2, \ldots, n \tag{A29}$$

Pick $x^{(1)}(1) = x^{(0)}(1)$, then:

$$\hat{x}^{(1)}(k+1) = \left(x^{(0)}(1) - \frac{\hat{b}}{\hat{a}}\right)e^{-\hat{a}(k)} + \frac{\hat{b}}{\hat{a}}, k = 2, \ldots, n \tag{A30}$$

The solution of $x^{(0)}(k)$ can be obtained by processing the inverse of $\hat{x}^{(1)}(k+1)$, which is:

$$\hat{x}^{(0)}(n) = \begin{cases} \hat{x}^{(0)}(1) = x^{(0)}(1) \quad n = 1 \\ \hat{x}^{(0)}(k) = \hat{x}^{(1)}(k) - \hat{x}^{(1)}(k-1) = (1-e^{a})\left(x^{(0)}(1) - \frac{b}{a}\right)e^{-a(k-1)} n = k \end{cases} \tag{A31}$$

Bringing in the data of rural residential land from 2000 to 2015, the fitted curve of rural settlement land in 31 provinces can be obtained. According to this fitting curve, the predicted value in 2020 can be obtained and compared with the real value in 2020, and it can be obtained that the error range of most of the 31 provinces is within 10%, with an average error of 7%, so it can be judged that this method is more credible for measuring urban land use. Table A1 shows the predicted and true values of rural residential land in 2020 and the error for each region.

Table A1. Predicted, real and error values of rural residential land use in 2020 in 31 provincial administrative regions.

	2020 Prediction	2020 Real	Error (%)
Beiijng (BJ)	1577.37	1577.37	−6.55371
Tianjin(TJ)	1120.68	1120.68	0.419123
Hubei(HB)	13,564.44	13,564.44	1.159223
Shanxi(SX)	4528.96	4528.96	3.590098
Inner Mongolia (NMG)	9989.20	9989.20	−1.76814
Liaoning (LN)	8105.94	8105.94	1.122002
Jilin (JL)	5571.41	5571.41	0.187167
Heilongjiang (HLJ)	7236.44	7236.44	−1.1415
Shanghai (SH)	733.53	829.10	26.58004
Jiangsu (JS)	11,654.78	11,654.78	−0.25006
Zhejiang (ZJ)	2984.22	2984.22	−0.05962
Anhui (AH)	11,377.71	11,377.71	1.189202
Fujian (FJ)	1577.14	1577.14	−1.36721
Jiangxi (JX)	2297.61	2297.61	−0.83703
Shandong (SD)	15,562.27	15,562.27	0.395245
Henan (HEN)	15,510.94	15,510.94	−0.82518
Hubei (HUB)	3799.61	3799.61	−0.71565

Table A1. *Cont.*

	2020 Prediction	2020 Real	Error (%)
Hunan (HUN)	1655.07	1655.07	−1.89245
Guangdong (GD)	4124.06	4124.06	−1.55022
Guangxi (GX)	3448.43	3448.43	0.07054
Hainan (HN)	545.55	545.55	−2.05527
Chongqing (CQ)	359.04	359.04	−3.48316
Sichuan (SC)	2337.59	2337.59	−1.74059
Guizhou (GZ)	305.93	305.93	−1.94585
Yunnan (YN)	1793.45	1793.45	1.958432
Tibet (XZ)	127.71	127.71	−14.2858
Shaanxi (SAX)	3058.29	3058.29	1.977146
Gansu (GS)	3419.72	3419.72	0.550511
Qinghai (QH)	691.49	691.49	1.990066
Ningxia (NX)	1133.61	1133.61	1.305904
Xinjiang (XJ)	4191.52	4191.52	16.26951

References

1. Qu, Y.; Wang, S.; Tian, Y.; Jiang, G.; Zhou, T.; Meng, L. Territorial spatial planning for regional high-quality development–An analytical framework for the identification, mediation and transmission of potential land utilization conflicts in the Yellow River Delta. *Land Use Policy* **2023**, *125*, 106462.
2. Liu, Y.; Zhou, Y. Territory spatial planning and national governance system in China. *Land Use Policy* **2021**, *102*, 105288. [CrossRef]
3. Kou, Z.; Liu, X. On Patenting Behavior of Chinese Firms: Stylized Facts and Effects of Innovation Policy. *Econ. Res. J.* **2020**, *55*, 83–99.
4. Liu, Y.; Fang, F.; Li, Y. Key issues of land use in China and implications for policy making. *Land Use Policy* **2014**, *40*, 6–12. [CrossRef]
5. Lu, S.; Wang, H. Limited Decentralization: Understand China's Land System from the Perspective of Central-Local Relation. *Land* **2022**, *11*, 517. [CrossRef]
6. Wu, S.; Yang, Z. Informal government preferences and asymmetric land allocation in China. *Land Use Policy* **2020**, *99*, 105085. [CrossRef]
7. Peng, Q.; Zhou, H. Chinese land complex: Hometown ties and corporate land acquisition. *Land Use Policy* **2024**, *138*, 107030. [CrossRef]
8. Guo, T. The State Planning Commission Promulgates the Compilation Measures for Territorial Planning. *Geogr. Territ. Res.* **1987**, *4*, 1–2.
9. Ding, C. Land policy reform in China: Assessment and prospects. *Land Use Policy* **2003**, *20*, 109–120. [CrossRef]
10. Li, B.; Wang, Z.; Chai, J.; Zhang, D. Index system to assess implementation of strategic land use plans in China. *Land Use Policy* **2019**, *88*, 104148. [CrossRef]
11. Zhou, Y.; Huang, X.; Zhong, T.; Chen, Y.; Yang, H.; Chen, Z.; Xu, G.; Niu, L.; Li, H. Can annual land use plan control and regulate construction land growth in China? *Land Use Policy* **2020**, *99*, 105026. [CrossRef]
12. Lin, J.; Wu, Y.; Wu, J.; Liu, S.Y. On the Construction of the Spatial Planning System: Also Analyzing the Relationships among Spatial Planning, Territorial Spatial Use Control, and Natural Resources Supervision. *City Plan. Rev.* **2018**, *42*, 9–17.
13. Yan, J.; Chen, H.; Xia, F. "Multi—Plan Integration" and Spatial Planning: Cognition, Orientation and Path. *China Land Sci.* **2017**, *31*, 21–27.
14. Diamond, J.; Wright, J. Design of an integrated spatial information system for multiobjective land-use planning. *Environ. Plan. B Plan. Des.* **1988**, *15*, 205–214. [CrossRef]
15. Dökmeci, V.; Berköz, L. Transformation of Istanbul from a monocentric to a polycentric city. *Eur. Plan. Stud.* **1994**, *2*, 193–205. [CrossRef]
16. Alam, M.; Elias, S.; Rahman, M. Optimum land use pattern and resource allocation in a growing economy: A closed model approach. *Bangladesh J. Agric. Econ.* **1995**, *18*, 15–37.
17. Storbeck, J. The Spatial Structuring of Central Places. *Geogr. Anal.* **2010**, *20*, 93–110. [CrossRef]
18. Aghakhani, S.; Rajabi, M. A New Hybrid Multi-Objective Scheduling Model for Hierarchical Hub and Flexible Flow Shop Problems. *Appl. Math* **2022**, *2*, 721–737. [CrossRef]
19. Veldkamp, A.; Fresco, L. CLUE: A conceptual model to study the conversion of land use and its effects. *Ecol. Model.* **1996**, *85*, 253–270. [CrossRef]
20. Verburg, P.; Soepboer, W.; Veldkamp, A.; Limpiada, R.; Espaldon, V.; Mastura, S.S.A. Modeling the spatial dynamics of regional land use: The CLUE-S model. *Environ. Manag.* **2002**, *30*, 391–405. [CrossRef]

21. Wei, W. Land use optimal allocation based on CLUE-S and MCR model in Shiyang River Basin. Ph.D. Thesis, Lanzhou University, Lanzhou, China, 2018.
22. Faris, J.; Beever, L.; Brown, M. Geography Information System (GIS) and Urban Land Use Allocation Model (ULAM) techniques for existing and projected land use data. In Proceedings of the Seventh National Conference on Transportation Planning for Small and Medium-Sized Communities, Little Rock, AR, USA, 28–30 September 2000; pp. 2000-9-28–2000-9-30.
23. Doelman, J.C.; Stehfest, E.; Tabeau, A.; van Meijl, H.; Lassaletta, L.; Gernaat, D.E.; Hermans, K.; Harmsen, M.; Daioglou, V.; Biemans, H.; et al. Exploring SSP land-use dynamics using the IMAGE model: Regional and gridded scenarios of land-use change and land-based climate change mitigation. *Glob. Environ. Change* **2018**, *48*, 119–135. [CrossRef]
24. Strengers, B.; Leemans, R.; Eickhout, B.; de Vries, B.; Bouwman, L. The land-use projections and resulting emissions in the IPCC SRES scenarios scenarios as simulated by the IMAGE 2.2 model. *GeoJournal* **2004**, *61*, 381–393. [CrossRef]
25. Peng, Y. Metropolitan Land Use Optimization Simulation Based on FLUS Model—Setting Shenzhen Cityas an Example. *Shandong Land Resour.* **2019**, *35*, 70–74.
26. Liu, X.; Li, X.; Liang, X.; Shi, H.; Ou, J.P. Simulating the Change of Terrestrial Carbon Storage in China Based on the FLUS-InVEST Model. *Trop. Geogr.* **2019**, *39*, 397–409.
27. Cao, K.; Huang, B.; Wang, S.; Lin, H. Sustainable land use optimization using Boundary-based Fast Genetic Algorithm. *Comput. Environ. Urban Syst.* **2012**, *36*, 257–269. [CrossRef]
28. Yuan, M.; Liu, Y. Land use optimization allocation based on multi-agent genetic algorithm. *Trans. Chin. Soc. Agric. Eng.* **2014**, *30*, 191–199.
29. Gao, Y.; Li, Q. A segmented particle swarm optimization convolutional neural network for land cover and land use classification of remote sensing images. *Remote Sens. Lett.* **2019**, *10*, 1182–1191. [CrossRef]
30. Liu, X.; Li, X.; Shi, X.; Huang, K.; Liu, Y. A multi-type ant colony optimization (MACO) method for optimal land use allocation in large areas. *Int. J. Geogr. Inf. Sci.* **2012**, *26*, 1325–1343. [CrossRef]
31. Walras, L. *Elements of Pure Economics*; Routledge: Oxfordshire, UK, 2013.
32. Johnson, R. Input-Output Models With and Without The Multiplier Effect. In *Valuing Tourism: Methods and Techniques*; Occasional Paper; Bureau of Tourism Research Canberra: Canberra, Australia, 1999; p. 28.
33. Parrado, R.; De Cian, E. Technology spillovers embodied in international trade: Intertemporal, regional and sectoral effects in a global CGE framework. *Energy Econ.* **2014**, *41*, 76–89. [CrossRef]
34. Lim, B.; Chang, J.; Choi, G.W.; Kim, S.A. Analysis of the International Trade and Ocean Economy in Korea Using a Computable General Equilibrium (CGE) Model. *J. Coast. Res.* **2024**, *116*, 378–382. [CrossRef]
35. Lemelin, A.; Savard, L. What do CGE models have to say about fiscal reform? *Econ. Anal. Policy* **2022**, *74*, 758–774. [CrossRef]
36. Xu, J.; Wei, W. Would carbon tax be an effective policy tool to reduce carbon emission in China? Policies simulation analysis based on a CGE model. *Appl. Econ.* **2022**, *54*, 115–134. [CrossRef]
37. Ghani, S.; Morgandi, N. Return migration and labour market outcomes in South Asia: A CGE exploration. *J. Ethn. Migr. Stud.* **2023**, *49*, 5153–5168. [CrossRef]
38. Zhang, Q.; Zhang, X.; Cui, Q.; Cao, W.; He, L.; Zhou, Y.; Li, X.; Fan, Y. The unequal effect of the COVID-19 pandemic on the labour market and income inequality in China: A multisectoral CGE model analysis coupled with a micro-simulation approach. *Int. J. Environ. Res. Public Health* **2022**, *19*, 1320. [CrossRef]
39. Darwin, R. A farmer's view of the Ricardian approach to measuring agricultural effects of climatic change. *Clim. Change* **1999**, *41*, 371–411. [CrossRef]
40. Burniaux, J.; Lee, H. Modelling Land Use Changes in GTAP. In Proceedings of the 6th Annual Conference on Global Economic Analysis, The Hague, The Netherlands, 12–14 June 2003.
41. Decreux, Y.; Valin, H. *MIRAGE, Updated Version of the Model for Trade Policy Analysis: Focus on Agriculture and Dynamics*; Working Paper; CEPII Research Center: Gainesville, FL, USA, 2007; p. 15.
42. Laborde, D.; Valin, H. Modeling land-use changes in a global CGE: Assessing the EU biofuel mandates with the MIRAGE-BioF model. *Clim. Change Econ.* **2012**, *3*, 1250017. [CrossRef]
43. Deng, X.; Yin, F.; Lin, Y.; Jin, Q.; Qu, R. Equilibrium analyses on structural changes of land uses in Jiangxi Province. *J. Food Agric. Environ.* **2012**, *10*, 846–852.
44. Yu, Z.; Deng, X.; Cheshmehzangi, A.; Mangi, E. Structural succession of land resources under the influence of different policies: A case study for Shanxi Province, China. *Land Use Policy* **2023**, *132*, 106810. [CrossRef]
45. Bento de Souza Ferreira Filho, J.; Ribera, L.; Horridge, M. Deforestation control and agricultural supply in Brazil. *Am. J. Agric. Econ.* **2015**, *97*, 589–601. [CrossRef]
46. Wang, C.; Siriwardana, M.; Meng, S. Effects of the Chinese arable land fallow system and land-use change on agricultural production and on the economy. *Econ. Model.* **2019**, *79*, 186–197. [CrossRef]
47. do Prado Tanure, T.; Miyajima, D.; Magalhães, A.S.; Domingues, E.P.; Carvalho, T.S. The impacts of climate change on agricultural production, land use and economy of the legal amazon region between 2030 and 2049. *EconomiA* **2020**, *21*, 73–90. [CrossRef]

48. China Statistical Yearbook-2018. Available online: https://www.stats.gov.cn/sj/ndsj/2018/indexch.htm (accessed on 24 October 2018).
49. Ministry of Ecology and Environment of the People's Republic of China. *China Environmental Statistics Yearbook*; China Statistics Press: Beijing, China, 2018; pp. 51–55.
50. National Bureau of Statistics of China. *China Population and Employment Statistics Yearbook*; China Statistics Press: Beijing, China, 2018; pp. 2–5.
51. National Bureau of Statistics of China. *China Rural Statistics Yearbook*; China Statistics Press: Beijing, China, 2018; pp. 50–51.
52. National Bureau of Statistics of China. *China Labour Statistics Yearbook*; China Statistics Press: Beijing, China, 2018; pp. 8–9.
53. Xu, X.; Liu, J.; Zhang, S.; Li, R.; Yan, C.; Wu, S. *China Multi-Period Land Use Remote Sensing Monitoring Data Set (CNLUCC)*; Resource and Environmental Science Data Platform: Beijing, China, 2018. Available online: http://www.resdc.cn/ (accessed on 2 July 2018). [CrossRef]
54. Feenstra, R.C.; Inklaar, R.; Timmer, M.P. The Next Generation of the Penn World Table. *Am. Econ. Rev.* **2015**, *105*, 3150–3182. [CrossRef]
55. China Issues National Plan on Population Development. Available online: https://english.www.gov.cn/policies/latest_releases/2017/01/25/content_281475551306587.htm (accessed on 1 January 2017).
56. World Health Statistics. Available online: https://www.who.int/data/gho/publications/world-health-statistics (accessed on 19 May 2022).
57. Fu, B.; Liu, Y.; Meadows, M. Ecological restoration for sustainable development in China. *Natl. Sci. Rev.* **2023**, *10*, nwad033. [CrossRef] [PubMed]
58. Lu, Y.; Cai, F. The impact of demographic change on potential growth rate: A comparison between China and Japan. *J. World Econ.* **2014**, *37*, 3–29.
59. Sheng, L.; Li, T.; Mao, S.Y.; Fu, L.H. Total Factor Productivity Measurement and Forecast of Economic Growth in China. *J. Stat. Inf.* **2018**, *33*, 3–11.
60. Qi, Z. A Simulation of the Necessary Total Factor Productivity Growth and Its Feasible Dual Circulation Source Pathways to Achieve China's 2035—Economic Goals: A Dynamic Computational General Equilibrium Study. *Sustainability* **2024**, *16*, 8237. [CrossRef]
61. Bailliu, J.; Kruger, M.; Toktamyssov, A.; Welbourn, W. How fast can China grow? The Middle Kingdom's prospects to 2030. *Pac. Econ. Rev.* **2019**, *24*, 373–399. [CrossRef]
62. Outline of National Overall Land and Spacial Planning 2016–2030. Available online: https://www.gov.cn/zhengce/content/2017-02/04/content_5165309.htm (accessed on 4 February 2017).
63. Yang, W.; Huang, R.; Li, D. China's high-quality economic development: A study of regional variations and spatial evolution. *Econ. Change Restruct.* **2024**, *57*, 86. [CrossRef]
64. Chen, S.; Wang, X.; Yao, S. National water-saving city and its impact on agricultural total factor productivity: A case study of nine provinces along the Yellow River, China. *J. Clean. Prod.* **2023**, *417*, 138019. [CrossRef]
65. Keola, S.; Andersson, M.; Hall, O. Monitoring economic development from space: Using nighttime light and land cover data to measure economic growth. *World Dev.* **2015**, *66*, 322–334. [CrossRef]
66. Yu, J.; Zhou, K.; Yang, S. Land use efficiency and influencing factors of urban agglomerations in China. *Land Use Policy* **2019**, *88*, 104143. [CrossRef]
67. Pang, J.; Zou, J. Computable general equilibrium (CGE) models and environmental policies anaylsis. *China Popul. Resour. Environ.* **2005**, *15*, 59–63.
68. Jin, G.; Chen, K.; Wang, P.; Guo, B.; Dong, Y.; Yang, J. Trade-offs in land-use competition and sustainable land development in the North China Plain. *Technol. Forecast. Soc. Change* **2019**, *141*, 36–46. [CrossRef]
69. Luo, J.; Zhan, J.; Lin, Y.; Zhao, C. An equilibrium analysis of the land use structure in the Yunnan Province, China. *Front. Earth Sci.* **2014**, *8*, 393–404. [CrossRef]
70. Lin, Y.; Deng, X.; Zhan, J. Simulation of regional land use competition for Jiangxi province. *Resour. Sci.* **2013**, *35*, 729–738.
71. Song, Q.; Jin, G. Land use modelling under the shared socioeconomic pathways: An empirical study of Hubei province based on CGE model. *J. Nat. Resour.* **2024**, *39*, 411–425. [CrossRef]
72. Wicke, B.; Verweij, P.; van Meijl, H.; van Vuuren, D.P.; Faaij, A.P. Indirect land use change: Review of existing models and strategies for mitigation. *Biofuels* **2012**, *3*, 87–100. [CrossRef]